applied sciences

MDPI

Article

Crystallization of Ag Nanoparticles in Borate–Bismuth Glass and Its Influence on Eu^{3+} Luminescence

Karolina Milewska [1,*], Michał Maciejewski [2], Marcin Łapiński [2], Anna Synak [3], Magdalena Narajczyk [4], Anna Bafia [2], Wojciech Sadowski [2] and Barbara Kościelska [2,*]

[1] Department of Built Environment and Energy Technology, Linnaeus University, 35195 Växjö, Sweden
[2] Faculty of Applied Physics and Mathematics, Institute of Nanotechnology and Materials Engineering, Gdańsk University of Technology, ul. Gabriela Narutowicza 11/12, 80-233 Gdańsk, Poland; michal.maciejewski@pg.edu.pl (M.M.); marcin.lapinski@pg.edu.pl (M.Ł.); s176465@student.pg.edu.pl (A.B.); wojciech.sadowski@pg.edu.pl (W.S.)
[3] Institute of Experimental Physics, Faculty of Mathematics, Physics and Informatics, University of Gdańsk, ul. Wita Stwosza 57/246, 80-952 Gdańsk, Poland; anna.synak@ug.edu.pl
[4] Bioimaging Laboratory, Faculty of Biology, University of Gdańsk, ul. Wita Stwosza 59, 80-952 Gdańsk, Poland; magdalena.narajczyk@biol.ug.edu.pl
* Correspondence: karolina.milewska@lnu.se (K.M.); barbara.koscielska@pg.edu.pl (B.K.)

Abstract: The aim of this study was to investigate the possibility of Ag nanoparticle crystallization in B_2O_3–Bi_2O_3 glass using a heat treatment method and to investigate the possible influence of the obtained nanoparticles on the emission intensity of Eu^{3+} ions. Borate–bismuth glasses with different B_2O_3:Bi_2O_3 molar ratios of 50:50, 60:40 and 70:50 with Ag and Eu^{3+} ions were successfully synthesized. The structure of the glasses was studied using XRD and FTIR methods. The XRD results exhibited a characteristic amorphous halo, confirming the absence of long-range order in the samples. The glass transition temperatures of various compositions, required to select the annealing temperature, were measured using DTA analysis. The strong maximum in the UV–Vis spectrum of the sample with the highest Bi_2O_3 content clearly indicated the presence of Ag nanoparticles in the glass. Moreover, a color change was observed for this sample, from slightly yellow to red. The presence of Ag nanoparticles was further confirmed via TEM and XPS studies. However, with a high content of Ag nanoparticles in the matrix, their positive effect on luminescence intensity was not observed. The obtained results show that B_2O_3–Bi_2O_3 glass and glass ceramics, with Ag nanoparticles and rare-earth (Re) ions, could be considered as a new phosphor for light-emitting diodes (LEDs).

Keywords: borate–bismuth glass; annealing; Ag nanoparticles; plasmon resonance; Eu^{3+} ions; luminescence; phosphors

check for updates

Academic Editors: Mioara Zagrai and Ramona-Crina Suciu

Received: 30 March 2025
Revised: 14 April 2025
Accepted: 16 April 2025
Published: 18 April 2025

Citation: Milewska, K.; Maciejewski, M.; Łapiński, M.; Synak, A.; Narajczyk, M.; Bafia, A.; Sadowski, W.; Kościelska, B. Crystallization of Ag Nanoparticles in Borate–Bismuth Glass and Its Influence on Eu^{3+} Luminescence. *Appl. Sci.* **2025**, *15*, 4495. https://doi.org/10.3390/app15084495

Copyright: © 2025 by the authors. Licensee MDPI, Basel, Switzerland. This article is an open access article distributed under the terms and conditions of the Creative Commons Attribution (CC BY) license (https://creativecommons.org/licenses/by/4.0/).

1. Introduction

Glasses doped with noble metal nanoparticles are a fascinating group of materials. The presence of nanoparticles in the glass matrix can significantly affect the optical properties of a material [1]. One of the most known effects of adding nanoparticles is the ability to control the optical properties of the material or even enhance the luminescence properties of rare-earth (Re) ions, which can lead to applications, e.g., in LEDs.

The presence of Ag nanoparticles in the glass matrix can lead to the occurrence of localized surface plasmon resonance (LSPR) phenomenon [2]. LSPR occurs when light interacts with nanoparticles smaller or similar in size to the incident light wavelength. As a result, the electrons of the conduction band oscillate coherently, creating surface plasmons

that propagate along the metal–insulator boundary as electromagnetic waves [3]. The LSPR results in enhancement of the electric field around the nanoparticle and its optical absorption, which is maximal at the plasmon resonant frequency. If Re ions are embedded in glass, and some of their energy levels are resonant with the plasmons, an enhancement of their luminescence properties can occur [4].

The formation of Ag nanoparticles can be obtained via a controlled crystallization process of glass using adequate heat treatment (HT) parameters, such as time and temperature [5]. The crystallization of nanoparticles in the glass matrix can occur slightly above the glass transition temperature (Tg) but lower than the first crystallization peak (Tc). In this temperature region, it is likely that silver ions can easily diffuse through glass, changing its valence state due to the one-step reduction process ($Ag^+ + 1e^- \rightarrow Ag^0$), and form nanoparticles via Ostwald ripening [3,5]. The formation of Ag nanoparticles in an amorphous matrix through thermal annealing has been described, in various glass compositions, such as Bi_2O_3–SiO_2–Ga_2O_3–Tm_2O_3–AgNO, TeO_2–BaO–Bi_2O_3, bismuth–germanate and K_2O–B_2O_3–Sb_2O_3 glasses [5–8].

The LSPR phenomenon, which enhances the luminescence properties of Re ions embedded in glass matrices, has been observed in various types of glasses, e.g., Er^{3+}/Yb^{3+} co-doped bismuth–germanate glasses containing silver NPs, $73TeO_2$–$4BaO$–$3Bi_2O_3$–$2Eu_2O_3$–Ag and Dy^{3+} doped boro-tellurite glasses with Ag nanoparticles [9,10]. It should be noted that in the case of glasses containing bismuth, one aspect can affect the formation of Ag nanoparticles. Eutectic transition has been reported between Ag and Bi_2O_3 [11]. According to the phase diagram by Assel et al., eutectic transformation can occur at around 687 ^{0}C, which is lower than the B_2O_3–Bi_2O_3 glass melting point [12]. The formation of (Bi_2O_3–Ag) eutectic was observed in Bi_2O_3–Ag bulk composite [13].

Borate–bismuth glass seems to be a good host for Ag nanoparticles. Boron oxide is a commonly used glass former in various types of commercial glasses with the ability to form glass in a wide range of Bi_2O_3 additions (20–80 mol% Bi_2O_3) [14,15]. The combination of boron and bismuth oxides results in their excellent optical properties, including a high refractive index and wide transparency for both visible and IR light [14,16,17]. Borate–bismuth glasses are also known for their good solubility for rare-earth (Re) ions, which makes them excellent hosts for them [18]. Moreover, they have high chemical and physical durability. Our prior experience with borate glasses demonstrates their efficacy as a matrix for luminescence applications when doped with bismuth oxide. So far, SrF_2 nanoparticles have been synthesized in B_2O_3–Bi_2O_3–Eu^{3+} glass using the heat treatment method, leading to enhanced luminescence of Eu^{3+} ions [19]. The enhancement of rare-earth ion luminescence was also achieved via modification of the basic borate–bismuth glass with AlF_3 while maintaining the transparency of the glass [20,21]. However, doping with Ag NPs has been successfully employed in fluoroborate B_2O_3–CaF_2 glasses with Eu^{3+} ions [22]. An enhanced luminescence caused by plasmon resonance was then observed. Silver nanoparticles were also successfully synthesized using the heat treatment method in sodium borate glasses doped with Er^{3+} ions [23]. The presence of Ag nanoparticles resulted in a significant enhancement of photoluminescence properties owing to the local field generated by Ag NPs. The suitability of borate glasses as a matrix for Ag nanoparticles was further confirmed by the results obtained for alkali borate-based glasses embedded with Nd^{3+} and silver nanoparticles [24]. The photoluminescence intensity spectra were enhanced due to the presence of silver nanoparticles.

The aim of this study was to investigate the possibility of Ag nanoparticle crystallization in B_2O_3–Bi_2O_3 glass using a heat treatment method and to investigate the possible influence of the obtained nanoparticles on the emission intensity of Eu^{3+} ions. Studies on the synthesis of Ag nanoparticles refer to matrices where B_2O_3 is either one of the

components in multicomponent glass or is associated with Ge_2O_3 or Si_2O_3. In this work, bismuth oxide was used as a component of borate glass. Due to the existence of eutectic between Bi_2O_3 and Ag, it should have a positive effect on the formation of nanoparticles in the matrix. To the best of our knowledge, there is no information on the synthesis of Ag nanoparticles in two-component B_2O_3–Bi_2O_3 glass. Due to the interesting properties of the proposed glass ceramics, borate–bismuth glasses with Ag nanoparticles are promising materials for Re ion luminescence enhancement and therefore for optical applications of such a material.

2. Experimental Section

For the purpose of silver and europium doping, three basic types of bismuth–borate glass matrices were proposed, with B_2O_3:Bi_2O_3 molar ratios of 50:50 (BBO(50:50)), 60:40 (BBO(60:40)) and 70:50 (BBO(70:30)). To such compositions, 1 mol% Ag and 0.5 mol% Eu_2O_3 (relative to the total composition of Bi and B) were added. The nominal compositions are reported in Table 1. Glasses were synthesized using conventional melt-quenching technique. Well-mixed starting raw materials (H_3BO_3, $Bi_5OH(OH)_9(NO_3)_4$, $Eu(NO_3)_3$ and $AgNO_3$) were melted in a porcelain crucible at 850 °C for 15 min. Afterward, the melts were poured onto a steel hot plate (~250 °C) and pressed by another plate immediately; they were then cooled down to room temperature. The as-prepared glasses were transparent, with a slightly yellow tint (Figure 1).

Table 1. Batch compositions (mol%) of the studied glasses.

Sample	B_2O_3	Bi_2O_3	Ag	Eu_2O_3
BBO(50:50)	50	50	-	-
BBO(60:40)	60	40	-	-
BBO(70:30)	70	30	-	-
BBO(50:50) + Ag	49.5	49.5	1	-
BBO(60:40) + Ag	59.5	39.5	1	-
BBO(70:30) + Ag	69.5	29.5	1	-
BBO(50:50) + Ag + Eu	49.25	49.25	1	0.5
BBO(60:40) + Ag + Eu	59.25	59.25	1	0.5
BBO(60:40) + Ag + Eu	69.25	29.25	1	0.5

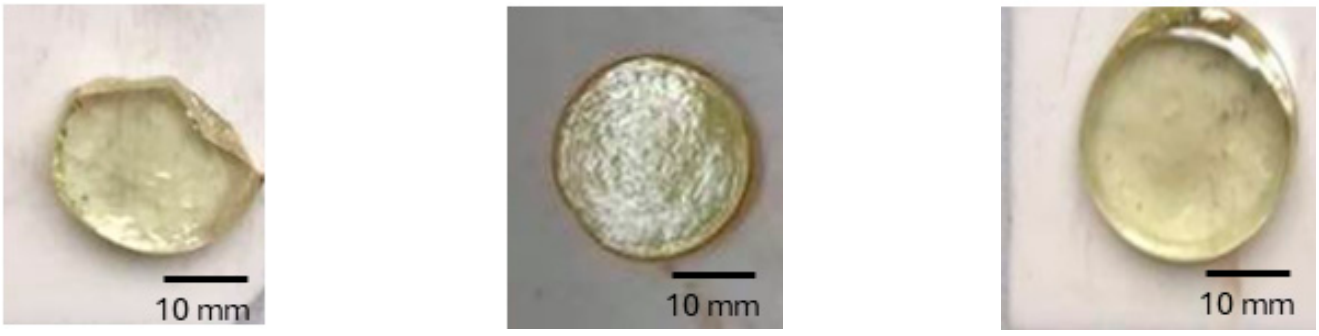

(**a**) (**b**) (**c**)

Figure 1. Photos of as-prepared glasses: (**a**) BBO(50:50) + Ag + Eu; (**b**) BBO(60:40) + Ag + Eu; (**c**) BBO(70:30) + Ag + Eu.

To investigate the formation of Ag nanoparticles in the glassy matrix, samples were annealed at 480 °C for 5 h in an air atmosphere. The interval was selected based on differential thermal analysis (DTA) studies, which were performed as follows.

Netzsch Simultaneous Thermal Analyzer STA 449 F1 Jupiter® (Netzsch, Selb, Germany) equipment was utilized for the analysis, with samples placed in a covered alumina

crucible (sample mass ~50 mg). The measurements were conducted in a synthetic air atmosphere at a controlled heating rate of 10 K/min. Calibration was performed to account for buoyancy effects, ensuring accurate thermal analysis for each sample within the temperature range of 45 °C–600 °C. Based on the collected data, the key thermal parameters, including glass transition temperature (Tg) and temperature at the beginning of the crystallization process (Tx) (the onset of the exothermic peak), were determined.

To obtain Ag nanoparticles, samples were annealed at three different temperatures: 450 °C, 480 °C and 500 °C, in the ΔT = Tx − Tg range. Among these, samples annealed at 480 °C for 5 h were selected for further luminescence analysis. The most noticeable change in color was observed in the BBO(50:50) + Ag sample (a photo of which is included in the figure showing the UV–Vis results). Samples annealed at 450 °C showed no change in color or transparency compared to unannealed samples. In contrast, the temperature of 500 °C turned out to be too high, as samples lost their transparency at this temperature.

The amorphous nature of the glasses was confirmed through X-ray diffraction (XRD) studies. The XRD measurements were conducted on powdered samples using a Philips X'PERT PLUS diffractometer (Philips, Amsterdam, The Netherland) with Cu-Kα radiation at room temperature.

To identify the structural units present in the samples, Fourier transform infrared spectroscopy (FTIR) was performed. The measurements were carried out using a Perkin-Elmer Frontier MIR/FIR spectrometer equipped with a TGS detector (Perkin-Elmer, Waltham, MA, USA). Pellet samples were prepared by mixing the material with potassium bromide (KBr) in a 1:100 weight ratio (sample:KBr).

UV–Vis spectra were recorded using a Perkin-Elmer Lambda 35 UV–Vis spectrophotometer (Perkin-Elmer, Waltham, MA, USA) within the wavelength range of 350–700 nm. The measurements were performed under argon atmosphere.

An X-ray photoelectron spectroscopy (XPS) analysis was conducted to determine the chemical state of silver nanoparticles present in the samples. The measurements were carried out using an Omicron NanoTechnology spectrometer (ScientaOmicron, Uppsala, Sweden) equipped with a 128-channel collector under ultra-high vacuum conditions ($<1.1 \times 10^{-8}$ mBar). Photoelectrons were excited using an Mg-Kα X-ray source, with the X-ray anode operating at 15 keV and 300 W. Binding energy calibration was achieved by referencing the C1s peak (285.0 eV). The XPS spectra were processed using CasaXPS software (Casa Software Ltd., ver. 2.3.23., Devon, UK).

Photoluminescence emission and excitation spectra were acquired using a SCINCO FluoroMate FS-2 fluorescence spectrometer. Pellet samples were prepared by mixing the material with potassium bromide (KBr) in a 1:1 weight ratio.

For the transmission electron microscopy (TEM), samples were placed on copper grids coated with a 2% collodion solution and carbon. Probes were examined using a Tecnai Spirit BioTWIN (FEI) electron microscope (FEI Company, Eindhoven, The Netherlands) at 120 kV.

3. Results and Discussion

3.1. DTA Analysis

To investigate the thermal properties and stability of the synthesized glasses, differential thermal analysis (DTA) measurements were conducted. The results are presented in Figure 2. It can be observed that the glass transition temperature is influenced by B_2O_3 content. The glass transition temperatures (Tg) are approximately 426 °C, 443 °C and 460 °C for the respective B_2O_3:Bi_2O_3 molar ratios of 50:50, 60:40 and 70:50. The onset of the exothermic peak (Tx) associated with the crystallization process of the matrix shifts toward higher temperatures with the increase in B_2O_3 amount only for B_2O_3:Bi_2O_3 molar

ratios of 70:50 and is as follows: 485 °C, 484 °C and 510 °C (for 50:50, 60:40 and 70:50 ratios, respectively). None of the tested glass compositions exhibit a high-intensity peak. Taking the difference between Tx and Tg in order to define the glass stability region, it can be concluded that the increased B_2O_3 content relative to Bi_2O_3 positively influences the thermal stability of glasses. These measurements were performed mainly to investigate the glass stability region, which is a critical parameter in the formation of Ag nanoparticles. Their synthesis typically occurs at temperatures below the first exothermic peak but above the glass transition temperature. Above Tg, glass properties such as viscosity and ion mobility undergo significant changes, promoting the agglomeration of Ag nanoparticles. Silver ion Ag^+ can be reduced to metallic silver Ag^0 through a one-step process ($Ag^+ + 1e^- \rightarrow Ag^0$), with a reduction potential of $E_0 = 0.7996$ V [5]. Moreover, this low-temperature annealing prevents crystallization of the glass matrix, as observed in B_2O_3–Bi_2O_3 glasses [19]. The synthesis of Ag nanoparticles was carried out within the temperature range between Tg and Tx at 450 °C, 480 °C and at the temperature at which (for the two compositions) the crystallization process had started: 500 °C. These temperatures should be sufficient to initiate the migration of Ag ions, leading to the formation of Ag nanoparticles.

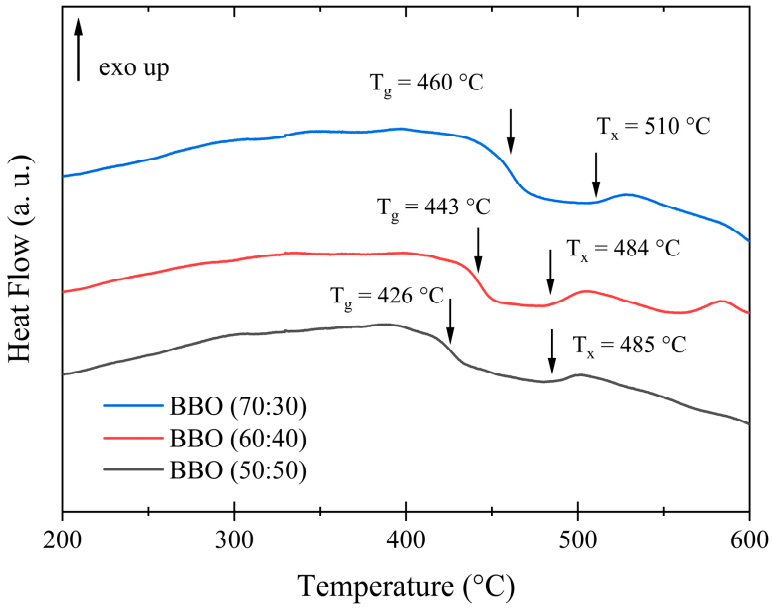

Figure 2. DTA curves of precursive glass compositions: BBO(50:50), BBO(60:40) and BBO(70:30). The characteristic Tg and Tc temperatures are marked with arrows.

3.2. XRD Analysis

Based on XRD measurements, the amorphous nature of the as-prepared glasses was confirmed. Similarly, glasses annealed at temperatures of 450 °C, 480 °C and 500 °C, proposed on the basis of DTA studies, are characterized by an amorphous structure. The exemplary diffraction patterns for unannealed samples and the BBO(50:50) + Ag, BBO(60:40) + Ag and BBO(70:30) + Ag samples annealed at 480 °C for 5 h are shown in Figure 3. Although bismuth–borate glass is very susceptible to crystallization, at least five stable crystalline phases can be observed [15,19,25,26], the broad maxima present in the 20–35 (2θ) and 40–55 (2θ) ranges indicate short-range ordering present in the samples. It was not possible to observe Ag nanoparticles in the glassy matrix due to the fact that only 1 mol% of silver was introduced into the samples.

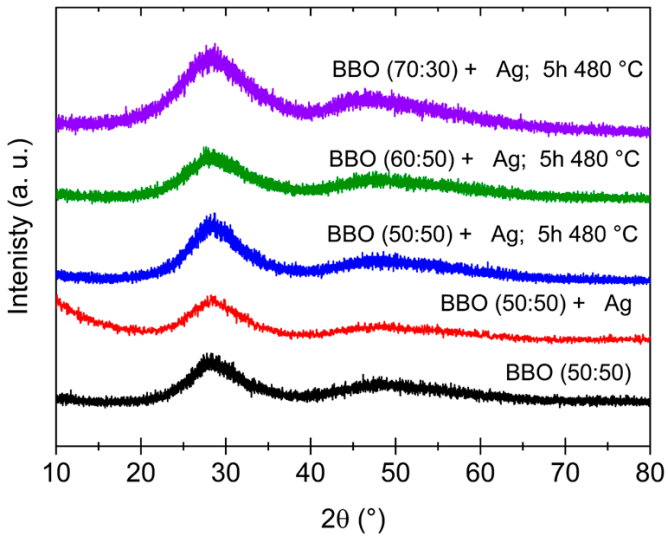

Figure 3. XRD patterns of as-prepared BBO(50:50) and BBO(50:50) + Ag samples and BBO(50:50) + Ag, BBO(60:40) + Ag and BBO(70:30) + Ag samples annealed at 480 °C for 5 h.

3.3. FTIR Analysis

As demonstrated in the results of FTIR studies, heating the glass at a temperature below Tc does not affect its internal structure. An exemplary comparison of the FTIR spectra of as-prepared BBO(50:50) and BBO(50:50) + Ag samples and BBO(50:50) + Ag samples annealed at 480 °C for 5 h is shown in Figure 4.

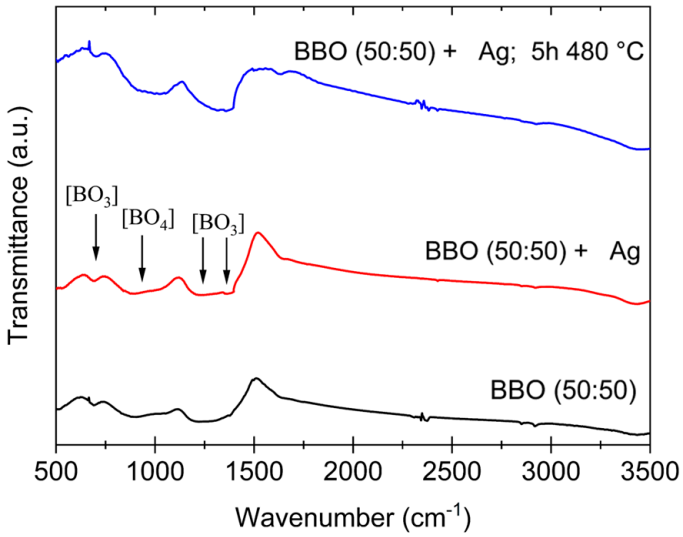

Figure 4. FTIR spectra of as-prepared BBO(50:50) and BBO(50:50) + Ag samples and BBO(50:50) + Ag samples annealed at 480 °C for 5 h.

It is well established that the borate glass network is primarily composed of [BO_3] triangular structural units, which can undergo transformation into [BO_4] tetrahedral units in the presence of a modifying agent. Such structural rearrangement may also be induced by Bi_2O_3 [15]. The broad absorption bands observed in the range of 680–720 cm^{-1} and 1100–1250 cm^{-1} are typically associated with the deformation and stretching vibrations of [BO_3] groups [26–28]. Also, a characteristic band appearing between 1200 and 1400 cm^{-1} corresponds to the stretching mode of the [BO_3] groups. Furthermore, the absorption band appearing at approximately 900–1100 cm^{-1} can be attributed to [BO_4] groups [27,28]. However, it is important to note that these bands may shift due to the influence of Bi_2O_3, and they may potentially overlap with the Bi_2O_3 peaks and shoulders [28]. Looking at the

spectra presented in Figure 5, it can be observed that neither the incorporation of Ag into the glass nor heating it below the crystallization temperature (Tc) had a significant effect on the spectra. Considering the DTA results, the chosen annealing temperature of 480 °C is well below the crystallization peak, and thus, it is not expected to induce any structural changes in the glass matrix. Additionally, the silver—introduced in very small quantities in the tested samples—did not alter the fundamental structural units of the glass.

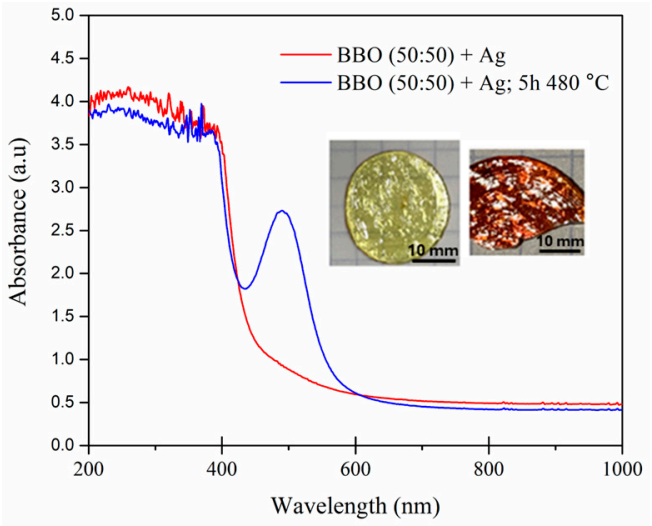

Figure 5. UV–Vis spectra of the BBO(50:50) + Ag as-prepared sample and the BBO(50:50) + Ag sample annealed at 480 °C for 5 h and photos of the as-prepared (light) and heated (red) samples.

3.4. UV–Vis Analysis

Although heating the samples at 480 °C for 5 h did not change their structure, their color clearly indicated the formation of silver nanoparticles in the matrix. This can be confirmed by the UV–Vis spectrum shown in Figure 5. The position of localized surface plasmon resonance (LSPR) strongly depends on the dielectric function of the host material which surrounds the nanoparticles [29,30]. Therefore, for example, the LSPR of silver nanoparticles in the air can be observed at a wavelength of approximately 400 nm [29], while the LSPR maximum of Ag nanoparticles in tellurite [2,31] or bismuth–germanate [8] glass matrix is red-shifted and observed at a wavelength of about 500 nm. Therefore, we can conclude that the peak at 500 nm observed in the borate–bismuth BBO(50:50) + Ag glass annealed at 480 °C for 5 h is related to the LSPR of Ag nanoparticles.

3.5. XPS Analysis

An XPS experiment was conducted to investigate the valence state of silver in a tellurite glass matrix. The representative spectrum of the BBO(50:50) + Ag sample, annealed at 480 °C for 5 h, is presented in Figure 6. The spectrum is highly noisy due to the low concentration of silver nanoparticles in the glass matrix. Despite this noise limitation, the Ag 3d core-level spectrum exhibits two distinct peaks, corresponding to Ag3d5/2 at ca. 368 eV and Ag 3d3/2 at 374 eV. These values and the spin–orbit splitting of 6 eV are consistent with the characteristic binding energies of silver [2,32]. However, analysis of only the Ag 3d spectrum provides limited information. In order to gain more comprehensive information on the valence state, it is necessary to reference the Auger electron spectrum and analyze the Wagner plot or calculate the Wagner parameter [2,33,34]. Based on the 3d photoelectron spectrum and the Auger electron plot, it could be concluded that the results indicate the presence of silver nanoparticles composed of pure metallic silver. Additionally, the survey spectrum indicates high sample purity, with no detectable contamination.

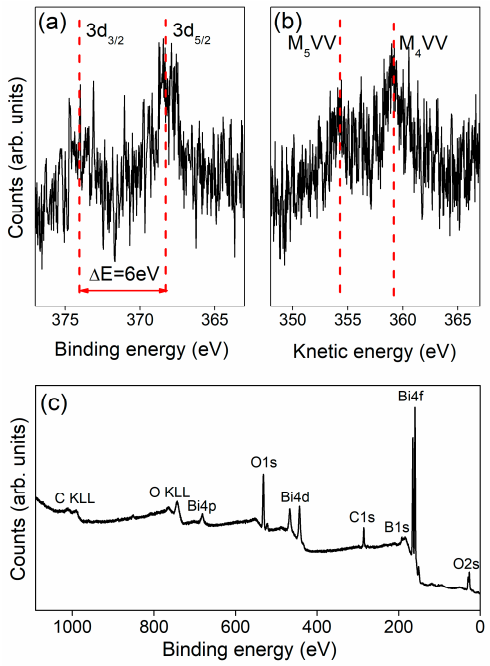

Figure 6. Ag3d photoelectron peaks (**a**), Auger lines (**b**) and survey spectrum (**c**) of the BBO(50:50) + Ag sample annealed at 480 °C for 5 h.

3.6. TEM Analysis

To confirm the presence of nanoparticles in the annealed borate–bismuth glass, TEM microscopy studies were performed. An exemplary image of the BBO(50:50) + Ag sample annealed at 480 °C for 5 h is presented in Figure 7. The shape of the nanoparticles is spherical, and they are rather randomly distributed in the glassy matrix. Taking into account the color change of the glass to red during annealing, the presence of an intense maximum in the UV–Vis spectrum, the results obtained via the XPS method and the TEM images, it can be clearly stated that the annealing of borate–bismuth glass led to the formation of silver nanoparticles in it. The diameters of the nanoparticles are approximately 2–5 nm, and they are randomly distributed in the glass.

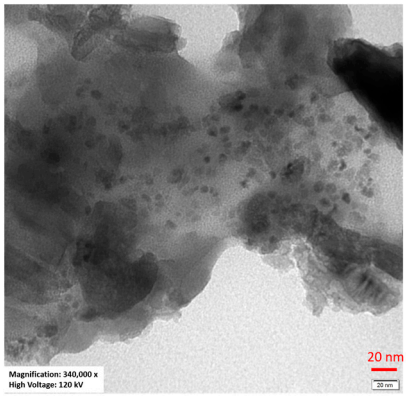

Figure 7. TEM image of the BBO(50:50) + Ag sample annealed at 480 °C for 5 h.

3.7. Photoluminescence

The excitation spectra of BBO(50:50) + Eu, BBO(60:40) + Eu and BBO(70:30) + Eu as-prepared samples monitored at 615 nm (Figure 8a–c, respectively) reveal several bands associated with the 4f–4f transitions of Eu^{3+}. They can be assigned to $^7F_0$–$^5D_4$ (362 nm), $^7F_0$–$^5G_2$ (382 nm), $^7F_0$–$^5L_6$ (395 nm), $^7F_1$–$^5D_3$ (415 nm) and $^7F_0$–$^5D_2$ (465 nm) transitions [35,36]. In the case of two glass compositions, two bands at 395 and 465 nm are characterized

by the highest intensity. The 454 nm wavelength line was selected in order to observe the emission spectra. The emission spectra of the as-prepared BBO(50:50) + Ag + Eu, BBO(60:40) + Ag + Eu and BBO(70:30) + Ag + Eu glasses and glasses annealed at 480 °C for 5 h are shown in Figure 8a–c, respectively. In all of them, several bands corresponding to Eu^{3+} radiative transitions are present: $^5D_0 \rightarrow {}^7F_0$ (578 nm), $^5D_0 \rightarrow {}^7F_1$ (591 nm), $^5D_0 \rightarrow {}^7F_2$ (615 nm), $^5D_0 \rightarrow {}^7F_3$ (652 nm) and $^5D_0 \rightarrow {}^7F4$ (700 nm). It was found that the electric dipole transition $^5D_0 \rightarrow {}^7F_2$ was the transition with the highest intensity for all samples.

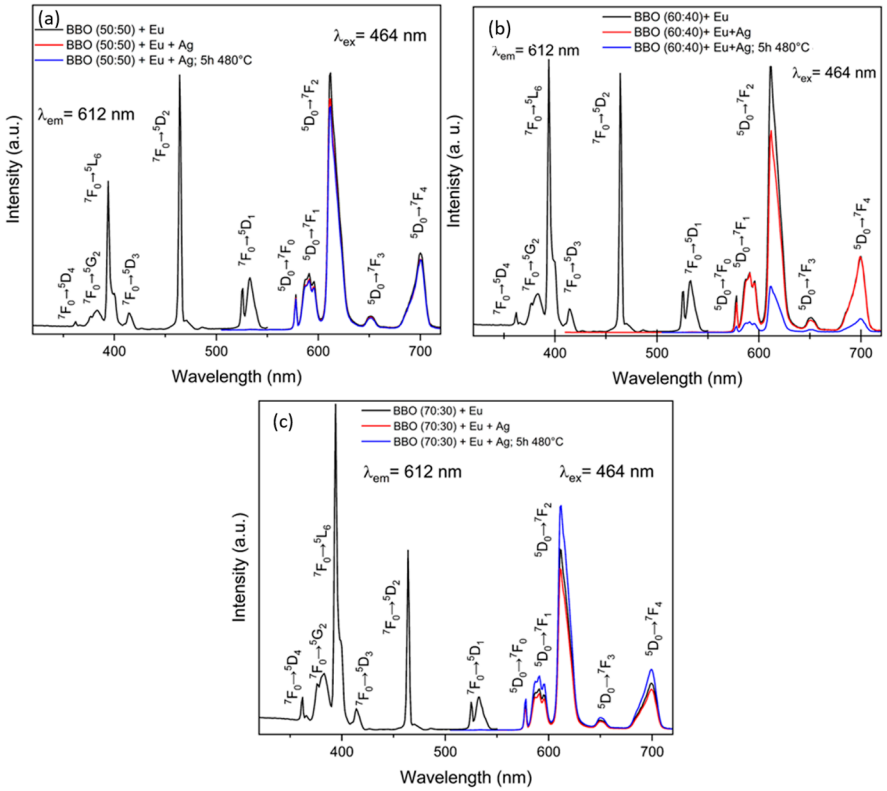

Figure 8. Excitation and emission spectra of as-prepared and annealed samples: (**a**) BBO(50:50) + Ag + Eu; (**b**) BBO(60:40) + Ag + Eu; (**c**) BBO(70:30) + Ag + Eu.

However, the positive effect of Ag nanoparticles on the emission of Eu^{3+} ions was not observed for all samples. Metallic NPs embedded in a glassy matrix near rare-earth ions can significantly influence the excitation and emission rates of these ions [37,38]. This effect is due to the enhancement of the local electromagnetic field around the nanoparticles caused by their localized surface plasmon resonance. As a result, energy transfer between the NPs and rare-earth ions can occur. However, the energy transfer can proceed in two directions: from metallic NPs to rare-earth ions, leading to an enhancement of luminescence intensity, and/or from rare-earth ions to NPs, resulting in luminescence quenching. The direction of the process depends on the concentration of metallic nanoparticles in the glassy matrix, or more precisely, on the ratio of the concentration of nanoparticles to Re ions [39,40]. If this ratio is greater than one, a reverse transfer from the ion to the nanoparticle will most likely occur, resulting in a decrease in luminescence intensity. Annealing had a positive effect on emission intensity only for the BBO(70:30) + Ag + Eu sample. It is possible that in this particular sample, where neither UV–Vis spectrum peak indicative of LSPR nor any color change of the sample after annealing were observed, a very small amount of nanoparticles was formed, and energy transfer from the nanoparticles to Eu^{3+} ions occurred, leading to an enhancement of luminescence. Meanwhile, in the other samples, a high concentration of nanoparticles had a negative effect, causing luminescence quenching due to reverse energy transfer from Eu^{3+} ions to Ag nanoparticles. Of course, further research would

be necessary to confirm the validity of the proposed explanation. Further research is also required in order to select the optimal glass composition at which the intensity of rare-earth ion luminescence would be maximal. Nevertheless, the obtained results show that borate–bismuth glasses are very promising materials for the manufacturing of silver nanostructures in them.

4. Conclusions

In summary, Ag nanoparticles in borate–bismuth glass were obtained via thermal annealing. Due to the existence of eutectic between Bi_2O_3 and Ag, an influence of Bi_2O_3 on the formation of Ag nanoparticles was observed, which was reflected in the color change of the glass with a high molar content of Bi_2O_3 (B_2O_3:Bi_2O_3 molar ratios of 50:50) during the annealing of the glass, from slightly yellow to red. In this sample, a strong absorption maximum on the UV–Vis spectrum was observed at a wavelength of about 500 nm, caused by the localized plasmon resonance of Ag nanoparticles. However, at a high content of Ag nanoparticles in the glass, quenching of the luminescence of Eu^{3+} ions took place, caused most probably by the energy transfer from Eu^{3+} ions to Ag nanoparticles. Selecting the most optimal glass composition at which the intensity of rare-earth ion luminescence would be maximal requires further research. The obtained results show that B_2O_3–Bi_2O_3 glass and glass ceramics, with Ag nanoparticles and rare-earth ions, could be considered as a new phosphor for light-emitting diodes (LEDs) [41,42].

Author Contributions: Conceptualization, B.K. and K.M.; methodology, B.K., K.M., M.M., M.Ł., W.S., M.N. and A.S.; formal analysis, K.M. and B.K.; data curation, K.M. and B.K.; writing—original draft preparation, K.M. and B.K.; writing—review and editing, B.K., K.M., M.M., M.Ł., W.S., M.N., A.S. and A.B.; supervision, B.K. All authors have read and agreed to the published version of the manuscript.

Funding: This research received no external funding.

Institutional Review Board Statement: Not applicable.

Informed Consent Statement: Not applicable.

Data Availability Statement: The raw data supporting the conclusions of this article will be made available by the authors on request.

Acknowledgments: The authors would like to thank Leon Murawski for fruitful discussions.

Conflicts of Interest: The authors declare no conflicts of interest.

Abbreviations

The following abbreviations are used in this manuscript:

XRD	X-Ray Diffraction
FTIR	Fourier Transform Infrared Spectroscopy
DTA	Differential Thermal Analysis
TEM	Transmission Electron Microscopy
XPS	Fourier Transform Infrared Spectroscopy
XPS	X-Ray Photoelectron Spectroscopy
LEDs	Light-Emitting Diodes
LSPR	Localized Surface Plasmon Resonance
HT	Heat Treatment
NPs	Nanoparticles

References

1. Wei, Y.; Ebendorff-Heidepriem, H.; Zhao, J. Recent Advances in Hybrid Optical Materials: Integrating Nanoparticles within a Glass Matrix. *Adv. Opt. Mater.* **2019**, *7*, 1900702. [CrossRef]
2. Lewandowski, T.; Dembski, M.; Walas, M.; Łapiński, M.; Narajczyk, M.; Sadowski, W.; Kościelska, B. Heat Treatment Effect on Eu^{3+} Doped TeO_2-BaO-Bi_2O_3 Glass Systems with Ag Nanoparticles. *J. Nanomater.* **2017**, *2017*, 5075326. [CrossRef]
3. Sutrisno, M.S.; Sabri, N.S.; Zaid, M.H.M.; Hisam, R. Tuning optical dispersion and localized surface plasmon resonance of 20Li2O-xBi2O3-(78-x)TeO2-1Er2O3-1Ag glass system. *Opt. Laser Technol.* **2023**, *157*, 108739. [CrossRef]
4. Mechergui, I.; Fares, H.; Mohamed, S.A.; Nalin, M.; Elhouichet, H. Coupling between surface plasmon resonance and Sm^{3+} ions induced enhancement of luminescence properties in fluoro-tellurite glasses. *J. Lumin.* **2017**, *190*, 518–524. [CrossRef]
5. Soltani, I.; Hraiech, S.; Horchani-Naifer, K.; Elhouichet, H.; Gelloz, B.; Férid, M. Growth of silver nanoparticles stimulate spectroscopic properties of Er^{3+} doped phosphate glasses: Heat treatment effect. *J. Alloys Compd.* **2016**, *686*, 556–563. [CrossRef]
6. Meng, S.; Zhao, G.; Hou, J.; Liu, Y.; Guo, Y.; Fang, Y.; Zhou, Y.; Zou, J. High performance of near-infrared emission for S-band amplifier from Tm^{3+}-doped bismuth glass incorporated with Ag nanoparticles. *J. Lumin.* **2020**, *224*, 117313. [CrossRef]
7. Qi, J.; Xu, Y.; Huang, F.; Chen, L.; Han, Y.; Xue, B.; Zhang, S.; Xu, T.; Dai, S. Photoluminescence of Ag nanoparticles and Tm 3+ ions in the bismuth germanate glasses for the blue light-excited W-LED. *J. Am. Ceram. Soc.* **2014**, *97*, 1471–1474. [CrossRef]
8. Wu, Y.; Shen, X.; Dai, S.; Xu, Y.; Chen, F.; Lin, C.; Xu, T.; Nie, Q. Silver nanoparticles enhanced upconversion luminescence in Er^{3+}/Yb^{3+} codoped bismuth-germanate glasses. *J. Phys. Chem. C* **2011**, *115*, 25040–25045. [CrossRef]
9. Som, T.; Karmakar, B. Nano silver: Antimony glass hybrid nanocomposites and their enhanced fluorescence application. *Solid State Sci.* **2011**, *13*, 887–895. [CrossRef]
10. Vijayakumar, R.; Nagaraj, R.; Suthanthirakumar, P.; Karthikeyan, P.; Marimuthu, K. Silver (Ag) nanoparticles enhanced luminescence properties of Dy3+ ions in borotellurite glasses for white light applications. *Spectrochim. Acta Part A Mol. Biomol. Spectrosc.* **2018**, *204*, 537–547. [CrossRef]
11. Digges, T.G.; Tauber, R.N. Structure of Bi-Ag eutectic alloy. *J. Cryst. Growth* **1971**, *8*, 132–134. [CrossRef]
12. Assal, J.; Hallstedt, B.; Gauckler, L.J. Experimental Phase Diagram Study and Thermodynamic Optimization of the Ag-Bi-O System. *J. Am. Ceram. Soc.* **1999**, *82*, 711–715. [CrossRef]
13. Sadecka, K.; Gajc, M.; Orlinski, K.; Surma, H.B.; Klos, A.; Jozwik-Biala, I.; Sobczak, K.; Dluzewski, P.; Toudert, J.; Pawlak, D.A. When eutectics meet plasmonics: Nanoplasmonic, volumetric, self-organized, silver-based eutectic. *Adv. Opt. Mater.* **2015**, *3*, 381–389. [CrossRef]
14. Oprea, I.I.; Hesse, H.; Betzler, K. Optical properties of bismuth borate glasses. *Opt. Mater.* **2004**, *26*, 235–237. [CrossRef]
15. Bobkova, N.M. Characteristics of the Structural State of Bismuth Ions in Bismuth-Borate Glasses. *Glass Ceram.* **2019**, *75*, 383–386. [CrossRef]
16. Joo, C.; Werner-Zwanziger, U.; Zwanziger, J.W. The ring structure of boron trioxide glass. *J. Non-Cryst. Solids* **2000**, *261*, 282–286. [CrossRef]
17. Bhemarajam, J.; Prasad, P.S.; Babu, M.M.; Özcan, M.; Prasad, M. Investigations on structural and optical properties of various modifier oxides (Mo = ZnO, CdO, BaO, and PbO) containing bismuth borate lithium glasses. *J. Compos. Sci.* **2021**, *5*, 308. [CrossRef]
18. Liu, Y.H.; Chen, Y.J.; Lin, Y.F.; Luo, Z.D.; Huang, Y.D. Effect of Bi_2O_3 on spectroscopic properties and energy transfer in Yb^{3+}-Er^{3+}-co-doped bismuth borate glasses for 1.5 μm optical amplifiers. *Opt. Mater.* **2008**, *30*, 1883–1888. [CrossRef]
19. Milewska, K.; Maciejewski, M.; Synak, A.; Łapiński, M.; Mielewczyk-Gryń, A.; Sadowski, W.; Kościelska, B. From Structure to Luminescent Properties of B_2O_3-Bi_2O_3-SrF_2 Glass and Glass-Ceramics Doped with Eu^{3+} Ions. *Materials* **2021**, *14*, 4490. [CrossRef]
20. Milewska, K.; Maciejewski, M.; Łapiński, M.; Synak, A.; Behrendt, M.; Sadowski, W.; Kościelska, B. Structural and luminescence properties of B_2O_3-Bi_2O_3-AlF_3 glass doped with Eu^{3+}, Tb^{3+} and Tm^{3+} ions. *J. Non-Cryst. Solids* **2023**, *605*, 122169. [CrossRef]
21. Milewska, K.; Maciejewski, M.; Žitňan, M.; Velázquez, J.J.; Galusek, D.; Sadowski, W.; Kościelska, B. Tunable emission and energy transfer of B_2O_3–Bi_2O_3–AlF_3 glass system doped with Eu^{3+}/Dy^{3+}. *J. Lumin.* **2024**, *269*, 120440. [CrossRef]
22. Naranjo, L.P.; de Araújo, C.B. Enhanced blue photoluminescence of B_2O_3-CaF_2 glass-ceramics containing silver nanoparticles. *J. Alloys Compd.* **2018**, *749*, 40–43. [CrossRef]
23. Sayyed, M.I.; Almousa, N.M.; Keshavamurthy, K.; Jagannath, G. Enhanced Er^{3+} photoluminescence in sodium borate glasses containing silver nanoparticles for photonic functionalities. *Opt. Mater.* **2022**, *134*, 113194. [CrossRef]
24. Keshavamurthy, K.; Gurushantha, K.; Sayyed, M.I.; Almousa, N.; Mahaboob Pasha, U.; Jagannath, G.; Ramesh, P. Silver nanoparticles improved infrared photoluminescence of Nd^{3+} doped sodium borate glasses. *Infrared Phys. Technol.* **2022**, *127*, 104451. [CrossRef]
25. Bajaj, A.; Khanna, A. Crystallization of bismuth borate glasses. *J. Phys. Condens. Matter* **2009**, *21*, 035112. [CrossRef]
26. Bobkova, N.M. Properties and Structure of Bismuth-Borate Glasses. *Glass Ceram.* **2016**, *72*, 360–365. [CrossRef]
27. Pascuta, P.; Pop, L.; Rada, S.; Bosca, M.; Culea, E. The local structure of bismuth borate glasses doped with europium ions evidenced by FTIR spectroscopy. *J. Mater. Sci. Mater. Electron.* **2008**, *19*, 424–428. [CrossRef]

28. Ali, A.A.; Rammahb, Y.S.; El-Mallawany, R.; Souri, D. FTIR and UV spectra of pentaternary borate glasses. *Measurement* **2017**, *105*, 72–77. [CrossRef]
29. Garcia, M.A. Corrigendum: Surface plasmons in metallic nanoparticles: Fundamentals and applications. *J. Phys. D Appl. Phys.* **2011**, *44*, 283001. [CrossRef]
30. Goldstein, A.N. *Handbook of Nanophase Materials*; CRC Press: Boca Raton, FL, USA, 1997.
31. Fares, H.; Elhouichet, H.; Gelloz, B.; Fèrid, M. Silver nanoparticles enhanced luminescence properties of Er^{3+} doped tellurite glasses: Effect of heat treatment. *J. Appl. Phys.* **2014**, *116*, 123504. [CrossRef]
32. Firet, N.J.; Blommaert, M.A.; Burdyny, T.; Venugopal, A.; Bohra, D.; Longo, A.; Smith, W.A. Operando EXAFS study reveals presence of oxygen in oxide-derived silver catalysts for electrochemical CO_2 reduction. *J. Mater. Chem. A* **2019**, *7*, 2597–2607. [CrossRef]
33. Shimabukuro, M.; Hiji, A.; Manaka, T.; Nozaki, K.; Chen, P.; Ashida, M.; Tsutsumi, Y.; Nagai, A.; Hanawa, T. Time-Transient Effects of Silver and Copper in the Porous Titanium Dioxide Layer on Antibacterial Properties. *J. Funct. Biomater.* **2020**, *11*, 44. [CrossRef] [PubMed]
34. Wagner, C.D.; Riggs, W.M.; Davis, L.E.; Moulder, G.F. *Handbook of X-Ray Photoelectron Spectroscopy*; Perkin–Elmer Corporation: Eden Prairie, MN, USA, 1979.
35. Mungra, M.; Steudel, F.; Ahrens, B.; Schweizer, S. Tm/Tb/Eu triple-doped lithium aluminoborate glass for white light genertion. *J. Lumin.* **2017**, *192*, 71–76. [CrossRef]
36. Malta, O.; Santa-Cruz, P.; Sá, G.; Gilberto, F.; Auzel, F. Fluorescence enhancement induced by the presence of small silver particles in Eu^{3+} doped materials. *J. Lumin.* **1985**, *33*, 261–272. [CrossRef]
37. Mawlud, S.Q. Optical Properties of Tellurite Glasses Embedded with Gold Nanoparticles. In *Tellurite Glass Smart Materials. Applications in Optics and Beyond*; El-Mallawany, R., Ed.; Part of Springer Nature 2018, Switzerland; Springer International Publishing: Berlin/Heidelberg, Germany, 2018; pp. 105–142.
38. Pan, Z.; Ueda, A.; Aga, R.; Burger, A.; Mu, R.; Morgan, S.H. Spectroscopic studies of Er^{3+} doped Ge-Ga-S lass containing silver nanoparticles. *J. Non-Cryst. Solids* **2010**, *356*, 1097–1101. [CrossRef]
39. Awang, A.; Ghoshal, S.K.; Sahar, M.R.; Reza Dousti, M.; Amjad, R.J.; Nawaz, F. Enhanced spectroscopic properties and Judd-Ofelt parameters of Er-doped tellurite glass: Effect of gold nanoparticles. *Curr. Appl. Phys.* **2013**, *13*, 1813–1818. [CrossRef]
40. Da Silva, D.S.; de Assumpcao, T.A.; Kassab, L.R.; de Araujo, C.B. Frequency upconversion in Nd^{3+} doped PbO-GeO_2 glasses containing silver nanoparticles. *J. Alloys Compd.* **2014**, *586*, S516–S519. [CrossRef]
41. Longato, A.; Picco, S.; Moro, L.; Buffolo, M.; De Santi, C.; Trivellin, N.; Meneghesso, G.; Meneghini, M.; Della Gaspera, E.; Guglielmi, M.; et al. Glass-ceramic composites for high-power white-light-emitting diodes. *Ceram. Int.* **2021**, *47*, 17986–17992. [CrossRef]
42. He, M.; Jia, J.; Zhao, J.; Qiao, X.; Du, J.; Fan, X. Glass-ceramics phosphors for solid state lighting: A review. *Ceram. Int.* **2021**, *47*, 2963–2980. [CrossRef]

Disclaimer/Publisher's Note: The statements, opinions and data contained in all publications are solely those of the individual author(s) and contributor(s) and not of MDPI and/or the editor(s). MDPI and/or the editor(s) disclaim responsibility for any injury to people or property resulting from any ideas, methods, instructions or products referred to in the content.